

Response of a frozen polynya to the motion of an underwater circular cylinder

H. Xiong^a, B. Y. Ni^a, A. A. Korobkin^b

a. College of Shipbuilding Engineering, Harbin Engineering University, Harbin, China

b. School of Engineering, Mathematics and Physics, University of East Anglia, United Kingdom

Email: a.korobkin@uea.ac.uk

1 Introduction

A polynya is a special marine area that remains ice-free or covered only by a thin layer of ice, despite being surrounded by thick sea ice during the winter, which is also identified as crucial habitat for seals^[1]. In nature, orcas move beneath the ice with undulating motions, generating waves that break through the ice layer, ultimately allowing them to prey on seals resting on the ice. Whether from the perspective of marine engineering applications or the study of animal behavior, it is essential to have a better understanding of the interactions between polynyas, water, and underwater objects. The linear problem of radiation of surface and flexural-gravity waves by a submerged cylinder for a ice floe or polynya with free surface was investigated by Sturova (2015)^[2]. It was shown that ice response essentially depends on the position of the submerged body relative to the elastic plate edges. A similar conclusion was drawn by Li et al. (2017)^[3]'s research, which investigated the interaction of water wave with a body floating in a polynya. It was shown that no matter how wide the polynya is, the effect of the ice sheet always exists. More recently, Yang et al. (2024)^[4] analytically considered the interaction between a uniform current with a circular cylinder submerged in a fluid. In the present paper, the response of a frozen polynya to the motion of an underwater circular cylinder is investigated.

2 Formulation of the problem

Two-dimensional unsteady problem of a circular cylinder moving in a liquid of infinite depth under a frozen polynya is considered. The problem is described within the Cartesian coordinate system $Ox'y'$, see Fig.1. A prime stands for dimensional variables. The parts of the ice, where $|x'| > L'$, are modelled as rigid boundary, and the interval $-L' < x' < L'$, $y = 0$ corresponds to a polynya covered with a thin ice, see Fig.1. The thickness of ice in the polynya is h_i and the rigidity is $D = Eh_i^3 / [12(1 - \nu^2)]$ where E is the Young modulus and ν is the Poisson ratio of the ice. The liquid is incompressible and inviscid. The rigid cylinder of radius a is placed at $t' = 0$ under the ice with the centre of the cylinder being at $x' = s'_0$, $y' = -h'_0$. The half-length L' of the polynya is comparable with the radius of the cylinder a . The cylinder starts to move impulsively towards the ice cover at $t' = 0$ with a constant acceleration at a certain angle β to the horizontal, see Fig.1. At $t' = t_c$ the cylinder achieves a speed V and continues its motion along a given trajectory with a given speed being of order of V . The coordinates of the cylinder centre are $x' = s'(t')$ and $y' = -h'(t')$, where $s'(t')$ and $h'(t')$ are given functions such that $s'(0) = s'_0$, $h'(0) = h'_0$, $ds'/dt' = V \cos \beta$ and $dh'/dt' = -V \sin \beta$ at $t' = t_c$. The liquid flow caused by the cylinder motion is assumed potential. The corresponding velocity potential $\varphi'(x', y', t')$ satisfies the Laplace equation in the flow region $\Omega'(t')$, the boundary conditions on the surface of the cylinder and on the ice/liquid interface, and decays in the far field. Note that the flow region depends on deflection of the ice cover in the polynya. The hydrodynamic pressure $p'(x', y', t')$ in the flow region is given by the nonlinear Bernoulli equation. It is convenient to introduce the moving polar coordinate ρ' , α , to formulate the boundary condition on the surface of the cylinder, where $x' = s'(t') + \rho' \cos \alpha$, $y' = -h'(t') + \rho' \sin \alpha$, $\rho' \geq a$ and $0 < \alpha < 2\pi$.

The problem is formulated in dimensionless variables, where t_c is taken as the time scale, a as the length scale, V as the velocity scale, and $p_{sc} = V a \rho_w / t_c$ as the scale of the hydrodynamic pressure. ρ_w is the water density. The shape of the ice plate in the polynya is described by the equation $y' = w'(x', t')$, $-L' < x' < L'$, where $w'(x', t')$ is the ice deflection. The ice deflection is governed by the equation of a thin elastic plate. The scale of the ice deflection w_{sc} is obtained by requiring balance between the order of the hydrodynamic pressure acting on the ice sheet, $V a \rho_w / t_c$, and the order of the bending term in the elastic plate equation, $D \partial^4 w' / \partial x'^4 = O(D w_{sc} / a^4)$, which gives $w_{sc} = \rho_w V a^5 / (D t_c)$. The dimensionless hydrodynamic pressure in the flow is given by the nonlinear Bernoulli equation,

$$p(x, y, t) = -\varphi_t - |\nabla \varphi|^2 V t_c / (2a) - g y t_c / V, \quad (1)$$

where g is the gravity acceleration and the dimensionless variables are denoted by the same symbols but without primes. We consider such conditions of the body motion and such elastic

characteristics of the ice plate that the problem is coupled with ice deflection being dependent on the hydrodynamic loads and the flow being dependent on the ice deflection through the kinematic condition on the ice/water interface,

$$V\varphi_y = w_t w_{sc}/t_c + \varepsilon V w_x \varphi_x \quad (y = \varepsilon w(x, t), -L < x < L), \quad (2)$$

where $\varepsilon = w_{sc}/a$. The flow under the ice depends on the ice deflection, which indicates the problem is coupled, if w_{sc}/t_c is of order of V . Without loss of generality, we set $w_{sc} = Vt_c$. Comparing this deflection scale with the scale which follow from the plate equation, we find that the problem is coupled if the duration of the acceleration stage is of the order of

$$t_c = \sqrt{\rho_w a^5 / D} = (a/c_i)(\rho_w/\rho_i)^{1/2}(a/h_i)^{3/2}[12(1-\nu^2)]^{1/2}, \quad (3)$$

where $c_i = \sqrt{E/\rho_i}$ is the speed of longitudinal waves in the ice, ρ_i is the ice density.

It is assumed in the present study that the conditions of the motions are such that the deflection scale, w_{sc} , is much smaller than the length scale of the problem, a . Then $\varepsilon = w_{sc}/a$ is a small parameter of the problem, $\varepsilon \ll 1$. This condition gives $Vt_c/a \ll 1$, which is satisfied for relatively small speeds of the cylinder, see (3),

$$V \ll c_i(\rho_i/\rho_w)^{1/2}(h_i/a)^{3/2}[12(1-\nu^2)]^{-1/2}. \quad (4)$$

The equations of the ice deflection and the flow under the ice at the leading order as $\varepsilon \rightarrow 0$ are obtained in the dimensionless variables by setting ε to zero. The resulting boundary value problem is linear and coupled. The dimensionless deflection of the elastic plate $w(x, t)$ is described at the leading order by the equation

$$\chi w_{tt} + w_{xxxx} = -\varphi_t - \gamma w \quad (y = 0, -L < x < L), \quad (5)$$

where $\chi = \rho_i h_i / (\rho_w a)$, $\gamma = \varepsilon g t_c / V$. The plate equation (5) is to be solved subject to the clamped edge conditions and initial conditions,

$$w(\pm L, t) = 0, \quad w_x(\pm L, t) = 0, \quad w(x, 0) = 0, \quad w_t(x, 0) = 0. \quad (6)$$

The velocity potential $\varphi(x, y, t)$ satisfies the following equations,

$$\nabla^2 \varphi = 0, \quad (7)$$

$$\varphi_\rho = \dot{s}(t) \cos \alpha - \dot{h}(t) \sin \alpha \quad (\rho = 1, 0 < \alpha < 2\pi), \quad (8)$$

$$\varphi_y = 0 \quad (y = 0, |x| > L), \quad \varphi_y = w_t \quad (y = 0, |x| < L), \quad (9)$$

$$\varphi = 0 \quad (x^2 + y^2 \rightarrow \infty). \quad (10)$$

The flow region at the leading order as $\varepsilon \rightarrow 0$ is the lower half-plane $y < 0$ with a circular hole in it, $\rho = 1$. The strains in the ice plate in the polynya are given by

$$\epsilon(x, t) = \pm \epsilon_{sc} w_{xx} \quad (-L < x < L), \quad (11)$$

where $\epsilon_{sc} = \varepsilon h_i / (2a)$ is the scale of the strains and the yield strain of the ice, $\epsilon_Y = 8 \times 10^{-5}$ from Brocklehurst et al.(2010)^[5] is selected in the present study.

3 Solution of the problem

The velocity potential in the fluid domain is decomposed as,

$$\varphi(x, y, t) = \dot{s}(t)\varphi_1(x, y, t) - \dot{h}(t)\varphi_2(x, y, t) + \varphi_3(x, y, t), \quad (12)$$

where

$$\nabla^2 \varphi_j = 0 \quad (j = 1, 2, 3) \quad \text{in } \Omega(t), \quad (13a)$$

$$\varphi_{1,\rho} = \cos \alpha, \quad \varphi_{2,\rho} = \sin \alpha, \quad \varphi_{3,\rho} = 0, \quad (\rho = 1, 0 < \alpha < 2\pi) \quad (13b)$$

$$\varphi_{j,y} = 0 \quad (j = 1, 2, 3, y = 0, |x| > L), \quad (13c)$$

$$\varphi_{j,y} = 0 \quad (j = 1, 2), \quad \varphi_{3,y} = w_t \quad (y = 0, |x| < L), \quad (13d)$$

$$\varphi_j = 0 \quad (j = 1, 2, 3, x^2 + y^2 \rightarrow \infty). \quad (13e)$$

It is known that the Neumann problem for the potential $\varphi_3(x, y, t)$ has the solution only if the mean deflection of the ice plate is zero, $\int_{-L}^L \partial \varphi_3 / \partial y(x, 0, t) dx = 0$. Based on Eq.(13d), the ice deflection is sought in the form,

$$w(x, t) = \sum_{n=1}^{\infty} a_n(t) (\psi_n(x) - c_n / (2L)). \quad (14)$$

where $\psi_n(x)$ are the so-called normal modes of the dry elastic plate and $a_n(t)$ are the principal coordinates of the modes, which are to be determined. $c_n = \int_{-L}^L \psi_n(x) dx$. The normal modes are non-zero solutions of the eigenvalue problem,

$$\frac{d^4 \psi_n}{dx^4} = \lambda_n^4 \psi_n(x) \quad (-L < x < L), \quad \psi_n(\pm L) = 0, \quad \frac{d\psi_n}{dx}(\pm L) = 0. \quad (15)$$

The functions $\psi_n(x)$ and the eigenvalues λ_n for even and odd modes can be found in Korobkin et al.(2014)^[6]. The functions $\psi_n(x)$ are orthonormal, $\int_{-L}^L \psi_n(x) \psi_m(x) dx = \delta_{nm}$, where $\delta_{nn} = 1$

and $\delta_{nm} = 0$ for $n \neq m$.

To solve the problem (5)-(6), it is convenient to introduce a new unknown function $u(x, t) = \sum_{n=1}^{\infty} U_n(t)\psi_n(x)$, where $-L < x < L$, and decompose the plate equation (5) as

$$\chi w_t + \varphi(x, 0, t) = u, \quad u_t = -w_{xxxx} - \gamma w. \quad (16)$$

The equations (13) for the potential $\varphi_3(x, y, t)$ show that the potential can be sought in the form

$$\varphi_3(x, y, t) = \sum_{n=1}^{\infty} \dot{a}_n(t)\varphi_{3n}(x, y, t), \quad (17)$$

where the series (14) has been used. Substituting Eq.(12) at $y = 0$ and the series for $u(x, t)$ and $w(x, t)$ in the system (16), and multiplying both sides of the obtained system by $\psi_m(x)$, $m \geq 1$ and integrating in x from $-L$ to L using the orthonormal condition, we obtain the matrix form of a system of ordinary differential equations

$$\vec{a}_t = [\chi(\mathbb{I} - \mathbb{C}) + \mathbb{S}]^{-1} (-\dot{s}\vec{M} + \dot{h}\vec{N} + \vec{U}), \quad \vec{U}_t = [-\mathbb{D} - \gamma(\mathbb{I} - \mathbb{C})]\vec{a}, \quad (18)$$

where $S_{nm} = \int_{-L}^L \varphi_{3n}(x, 0, t)\psi_m(x)dx$, $M_m = \int_{-L}^L \varphi_1(x, 0, t)\psi_m(x)dx$, $N_m = \int_{-L}^L \varphi_2(x, 0, t)\psi_m(x)dx$. $\vec{a} = (a_1, a_2, a_3, \dots)^T$ is the vector of unknown coefficients in (14), \mathbb{I} is the unit matrix, \mathbb{C} is a matrix with the elements $C_{mn} = c_m c_n / (2L)$, \mathbb{S} is the added-mass matrix with elements S_{mn} , \mathbb{D} is diagonal matrix, $\mathbb{D} = \text{diag}(\lambda_1^4, \lambda_2^4, \lambda_3^4, \dots)$, \vec{M} , \vec{N} and \vec{U} are vectors which depend on the prescribed position of the cylinder $s(t)$, $h(t)$. Eqs. (18) are solved numerically with the initial conditions

$$\vec{a} = \vec{0}, \quad \vec{U} = \vec{0} \quad (t = 0). \quad (19)$$

The boundary value problems (13) for $j = 1, 2, 3$ are solved by using the conformal mapping

$$(z - s(t))/\mu = i + 2/(\zeta + i), \quad (20)$$

which maps the ring $R < |\zeta| < 1$ in the ζ - plane onto the flow region $\Omega(t)$ in the z - plane. Here $\mu = \sqrt{h^2 - 1}$, $R = h(t) - \mu$, $z = x + iy = s(t) - ih(t) + \rho e^{i\alpha}$ in the Cartesian x, y and the local polar ρ, α coordinates, $\zeta = \xi + i\eta = -ire^{i\theta}$, where $-\pi < \theta < \pi$, see Xiong et al.(2024)^[7] for details. In the ζ - plane of the conformal mapping, the decomposition (12) yields

$$\phi(r, \theta, t) = \dot{s}(t)\phi_1(r, \theta, t) - \dot{h}(t)\phi_2(r, \theta, t) + \phi_3(r, \theta, t), \quad (21)$$

where $\phi_j(r, \theta, t) = \varphi_j(x(r, \theta, t), y(r, \theta, t), t)$ $j = 1, 2, 3$. $\phi_j(r, \theta, t)$ can be solved within the corresponding boundary value problem of Eqs. (13),

$$\phi_1(r, \theta, h) = -2\mu \sum_{n=1}^{\infty} \varphi_n(r^n + r^{-n}) \sin(n\theta), \quad \phi_2(r, \theta, h) = 2\mu \sum_{n=1}^{\infty} \varphi_n [(r^n + r^{-n}) \cos(n\theta) - 2] \quad (22)$$

where $\varphi_n = R^{2n}/(1 - R^{2n})$, see Xiong et al.(2024)^[7]. The series (14) and (17) suggest the velocity potential $\phi_3(r, \theta, t)$ of the form

$$\phi_3(r, \theta, t) = \mu \sum_{n=1}^{\infty} \dot{a}_n(t)\Psi_n(r, \theta, t), \quad (23)$$

where

$$\Psi_n(r, \theta, t) = \sum_{j=0}^{\infty} (C_{nj} \cos(j\theta) + D_{nj} \sin(j\theta)) (r^j + R^{2j}/r^j), \quad (24)$$

$C_{nj} = \frac{1}{\pi j(1-R^{2j})} \int_{\theta^L}^{\theta^R} \frac{\psi_n(x(1, \theta, t)) - c_n/(2L)}{1 - \cos \theta} \cos(j\theta) d\theta$, $D_{nj} = \frac{1}{\pi j(1-R^{2j})} \int_{\theta^L}^{\theta^R} \frac{\psi_n(x(1, \theta, t)) - c_n/(2L)}{1 - \cos \theta} \sin(j\theta) d\theta$, $C_{n0} = -\sum_{j=1}^{\infty} (1 + R^{2j}) C_{nj}$, D_{n0} can be set zero. The angle $\theta^L(t)$ and $\theta^R(t)$ are solutions of the equations

$$x(1, \theta^L(t), t) = -L, \quad x(1, \theta^R(t), t) = L, \quad (25)$$

The first term in the Right-hand side of formula (5) for the hydrodynamic pressure along the ice/water interface represents the dynamic component of the pressure, $p_d(x, t)$, where

$$p_d(x, t) = -\varphi_t = -\phi_t - \phi_{\theta} x_t / x_{\theta} \quad (y = 0, -L < x < L). \quad (26)$$

4 Numerical results and discussion

The numerical results are presented in terms of the dynamic pressure, ice deflections and strains caused by the motion of the cylinder. Calculations are performed for the following reference values of the parameters, $\rho_i = 917 \text{ kg/m}^3$, $E = 4.2 \times 10^9 \text{ N/m}^2$, $\nu = 0.3$, $h_i = 0.1 \text{ m}$, $g = 9.81 \text{ m/s}^2$, $\rho_w = 1000 \text{ kg/m}^3$, $V = 2 \text{ m/s}$, $a = 0.5 \text{ m}$, $h'_0 = 1.5 \text{ m}$, $\beta = \pi/4$, and half-length $L' = 1 \text{ m}$. The integrals in Section 3 are numerically solved by using the same procedure as Xiong et al.(2024)^[7] did. The series of (14) are truncated by N terms and the system (18) is numerically solved by fourth

order Runge-Kutta method with dimensionless time step $\Delta t = 10^{-5}$. $N = 60$ was found to provide accurate solutions. It is convenient to introduce a parameter σ referring to the horizontal position of the centre of the cylinder to the left hand side of the polynya, as shown in Fig.2. σ are selected as $\sigma = -3, -2, -1, -0.5, 0, 1$ and 2 . In fact, the strains distributed along the upper surface of the polynya reach the yield strain ϵ_Y at the very beginning of the acceleration stage. The subsequent analysis concentrates mainly on the process from the initial moment until the strain reaches the yield value. Fig.3 shows the dimensionless maximum dynamic pressure of the cases with different σ corresponding to Fig.2. Fig.4 shows the ratio of the strains distributed along the upper surface to the yield strain at the time instant when the maximum strain reach the yield value for $\sigma = -3, \sigma = -0.5$ and $\sigma = 2$. $\sigma = -0.5$ is a special position of the cylinder, see Fig.3. At the initial moment, the maximum pressure increases with decreasing σ in the range $-0.5 < \sigma < 2$ and decreases with increasing σ in the range $-3 < \sigma < -0.5$. Additionally, the time it takes for the strains of polynya to reach ϵ_Y is shortest at $\sigma = -0.5$, among the cases considered. Furthermore, the strains at the boundaries of the polynya reaches ϵ_Y earlier than in the central region, as shown in Fig.4. More results and discussions will be presented at the workshop.

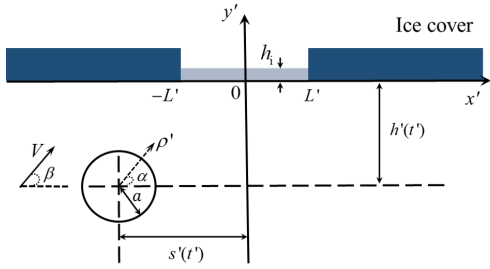


Figure 1: Sketch of the problem and notations

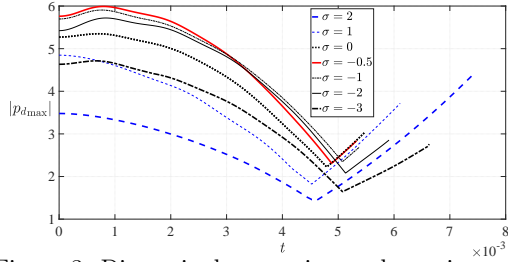


Figure 3: Dimensionless maximum dynamic pressure

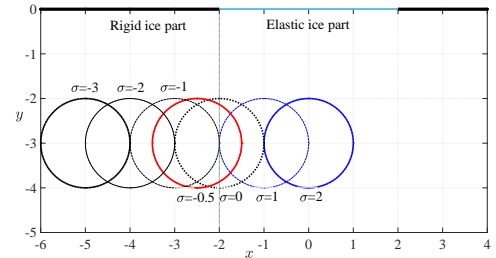


Figure 2: Position of the cylinder at each selected σ

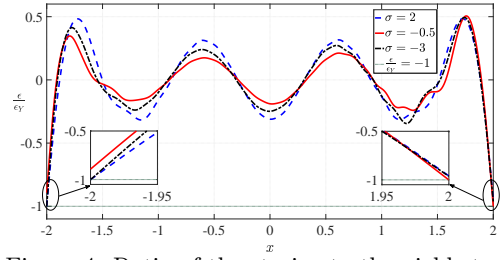


Figure 4: Ratio of the strains to the yield strain

5 Acknowledgement

This work was supported by the National Natural Science Foundation of China (Grants No.52192693, 52192690, 52371270, U20A20327, and 52350410468), the National Key Research and Development Program of China (Grant No.2021YFC2803400), and the Natural Science Foundation of Heilongjiang Province (Grant No.JJ2021TD0031).

6 References

- [1] Labrousse, S., Williams, G., Tamura, T., Bestley, S., Salle, J. B., Fraser, A. D., Sumner, M., Roquet, F., Heerah, K., Picard, B., Guinet, C., Harcourt, R., McMahon, C., Hindell, M. A. and Charrassin, J. B., 2018. Coastal polynyas: winter oases for subadult southern elephant seals in East Antarctica. *Scientific Reports*, 8, (1):3183.
- [2] Sturova, I.V., 2015. Radiation of waves by a cylinder submerged in water with ice floe or polynya. *Journal of Fluid Mechanics*, 784, 373C395.
- [3] Li, Z. F., Shi, Y. Y. and Wu, G. X., 2017. Interaction of wave with a body floating on a wide polynya. *Physics of Fluids*, 29, 097104.
- [4] Yang, Y. F., Wu, G. X. and Ren, K., 2024. Interaction between a uniform current and a submerged cylinder in a marginal ice zone. *Journal of Fluid Mechanics*, 984, A50.
- [5] Brocklehurst, P., Korobkin, A. A. and Părău, E. I., 2010. Interaction of hydro-elastic waves with a vertical wall. *Journal of Engineering Mathematics*, 68, (5), 215-231.
- [6] Korobkin, A. A., Khabakhpasheva, T. I. and Papin, A. A. 2014 Waves propagating along a channel with ice cover. *European Journal Of Mechanics B-fluids*, 47, 166-175.
- [7] Xiong, H., Ni, B. Y., Semenov, Y. and Korobkin, A. A., 2024. *Inertial motion of a circular cylinder approaching obliquely an ice cover*. [Submitted to Scientific Reports].